

LETTER TO THE EDITOR

Open Access



t(15;21) translocations leading to the concurrent downregulation of *RUNX1* and its transcription factor partner genes *SIN3A* and *TCF12* in myeloid disorders

Alberto L'Abbate^{1†}, Doron Tolomeo^{1†}, Francesca De Astis¹, Angelo Lonoce¹, Crocifissa Lo Cunsolo², Dominique Mühlematter³, Jacqueline Schoumans³, Peter Vandenberghe⁴, Achilles Van Hoof⁵, Orazio Palumbo⁶, Massimo Carella⁶, Tommaso Mazza⁷ and Clelia Tiziana Storlazzi^{1*}

Abstract

Through a combined approach integrating RNA-Seq, SNP-array, FISH and PCR techniques, we identified two novel t(15;21) translocations leading to the inactivation of *RUNX1* and its partners *SIN3A* and *TCF12*. One is a complex t(15;21)(q24;q22), with both breakpoints mapped at the nucleotide level, joining *RUNX1* to *SIN3A* and *UBL7-AS1* in a patient with myelodysplasia. The other is a recurrent t(15;21)(q21;q22), juxtaposing *RUNX1* and *TCF12*, with an opposite transcriptional orientation, in three myeloid leukemia cases. Since our transcriptome analysis indicated a significant number of differentially expressed genes associated with both translocations, we speculate an important pathogenetic role for these alterations involving *RUNX1*.

Keywords: Haploinsufficiency, Tumor suppressor genes, AML, MDS

Main text

Translocations involving *RUNX1* are known to decrease the function of the encoded protein in myelodysplastic syndromes (MDS) and acute myeloid leukemia (AML) [1]. For those involving chromosome 15, *SV2B* was the only *RUNX1* partner gene identified in AML [2].

We report on two novel t(15;21) alterations leading to the concurrent disruption of *RUNX1* and *SIN3A* or *TCF12* (Additional file 1: Table S1). Another interrupted gene is the *UBL7-AS1* long noncoding RNA gene.

In case 1, FISH experiments (Additional file 2: Table S2) mapped the breakpoint on der(21) within intron 7 of *RUNX1* (Additional file 3: Figure S1A-C). Moreover, SNP array analysis identified a 908-kb deletion near the 15q breakpoint on der(15) (Additional file 4: Table S3 and Additional file 3: Figure S1D-F). Genomic PCR revealed that intron 7 of *RUNX1* (chr21:36194775) was joined at intron 3 of *SIN3A* (chr15:75708434) (Fig. 1a and

Additional file 5: Table S4) on der(21). Furthermore, intron 7 of *RUNX1* (chr21:36194861) was fused to the inverted sequence of *UBL7* (NM_032907.4) at intron 1 (chr15:74751664) on der(15), suggesting that a sub-microscopic inversion accompanying the translocation led to the juxtaposition of *RUNX1* and *UBL7-AS1* with the same transcriptional orientation (Fig. 1a). ChimeraScan analysis of RNA-Seq data identified the fusion of *SIN3A* (exon 3; NM_015477) to *RUNX1* (exon 8; NM_001754) and of *RUNX1* (exon 7; NM_001754) to *UBL7-AS1* (intron 1; NR_038449.1). Both chimeric transcripts were validated by RT-PCR (Fig. 1b and Additional file 6: Table S5). In silico translation of the in-frame 5'-*SIN3A*/3'-*RUNX1* showed two ORFs of 171 and 163 amino acids, respectively, the first one retaining the transactivation domain of *RUNX1* (Fig. 1c). The out-of-frame 5'-*RUNX1*/3'-*UBL7-AS1* encoded a protein of 373 amino acids, showing the substitution of Runx1 with a GVQW putative binding domain (Fig. 1d). Thus, both chimeric *SIN3A*/*RUNX1* and *RUNX1*/*UBL7-AS1* encoded for truncated *SIN3A* and *RUNX1* proteins. Interestingly, RT-qPCR revealed that the full-length *RUNX1* (NM_001754) and the 3' portion of

* Correspondence: cleliatiziana.storlazzi@uniba.it

†Equal contributors

¹Department of Biology, University of Bari, Bari, Italy

Full list of author information is available at the end of the article

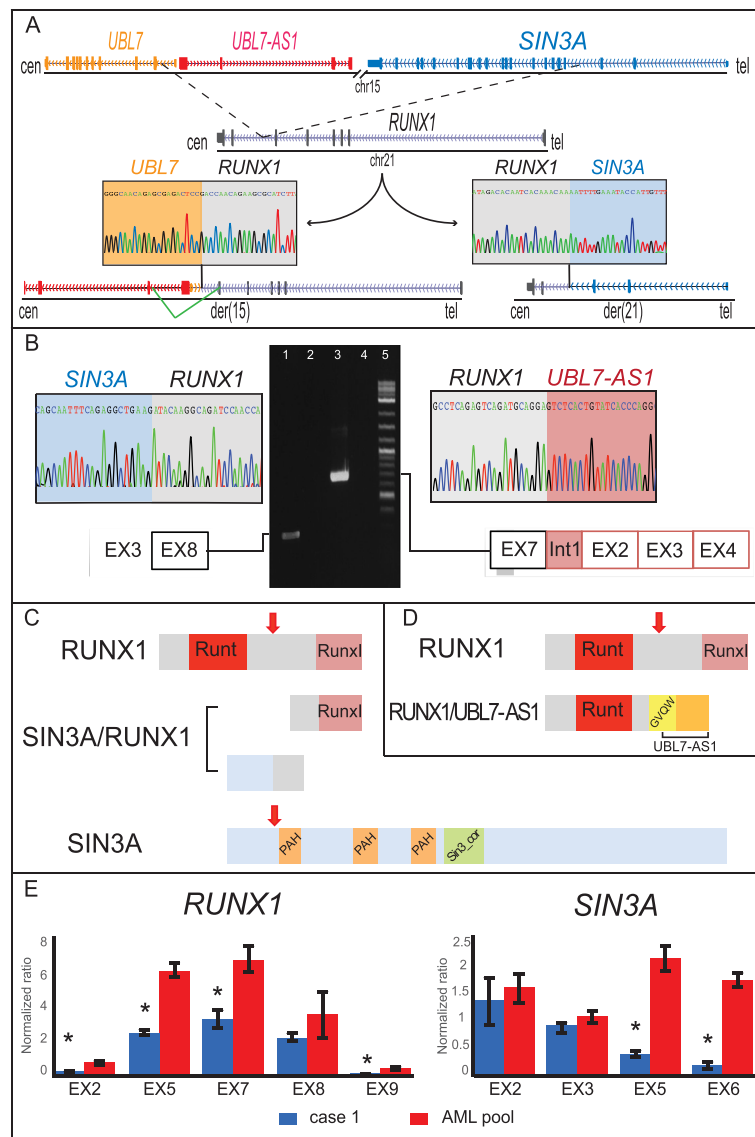


Fig. 1 t(15;21)(q24;q22) translocation in case 1. **a** Genomic breakpoints on chromosomes 15 and 21 in case 1: Top, schematic representation of wild-type chromosomes (black lines) and involved genes (exons are shown as rectangles and introns as lines connecting exons, with arrowheads indicating the direction of transcription). The dashed black lines indicate the breakpoints within all genes. Bottom, partial chromatograms indicate fusion sequences on der(15) (left) [GenBank: KT336107] and der(21) (right) [GenBank: KT336106]. The splicing event creating the runt-related transcription factor 1 (*RUNX1*)/*UBL7-AS1* fusion transcript is indicated in green. **b** *RUNX1* fusion transcripts: reverse transcription polymerase chain reaction (RT-PCR) products corresponding to *SIN3A/RUNX1* [GenBank: KT336104] and *RUNX1/UBL7-AS1* [GenBank: KT336105] fusion transcripts (lanes 1 and 3, respectively) in case 1 are shown in the middle of the panel. Lanes 2 and 4: negative normal bone marrow samples. Lane 5: 2-log DNA ladder (New England Biolabs, Milan, Italy). Partial chromatograms (top) and structure (bottom) of *SIN3A/RUNX1* and *RUNX1/UBL7-AS1* PCR products are on the left and on the right, respectively. **c, d** *RUNX1* chimeric proteins: both panels show in silico translation (ORFfinder and BlastP) of both wild-type and chimeric *RUNX1* and *SIN3A* proteins. Arrows indicate the truncation breakpoints of wild-type proteins. **e** Evaluation of *RUNX1* and *SIN3A* expression levels in case 1: exon-specific reverse transcription quantitative PCR analysis of *RUNX1* (left) and *SIN3A* (right) was performed in case 1 vs a control pooled sample of patients with acute myeloid leukemia. Asterisks indicate statistically significant results ($P < .05$)

SIN3A (NM_015477) were downregulated (Fig. 1e), whereas *UBL7-AS1* was overexpressed (Additional file 7: Figure S2). Further, we evaluated the molecular impact of these fusion transcripts through a differential expression analysis, using the control datasets of 19 AML cases with normal karyotype from the The Cancer Genome

Atlas data bank (<http://cancergenome.nih.gov/>). The results obtained by the QIAGEN's Ingenuity® Pathway Analysis (IPA®, QIAGEN Redwood City) [3], following the Partek Genomics Suite 6.6 (Partek Inc., St. Louis, MO, USA), indicated a significant number of differentially expressed genes within the AML pathway. The cell proliferation

and myeloid differentiation pathways were significantly activated, whereas apoptosis exhibited reduced activity (Additional file 8: Figure S3 and Additional file 9: Table S6).

The results obtained in case 1 clearly suggest a role as a tumor suppressor (TS) gene not only for *RUNX1* (the shorter *RUNX1* encoded by the chimeric *RUNX1/UBL7-AS1* should behave as a dominant negative mutant of the wild-type *RUNX1*), but also for *SIN3A*. We speculate that the inactivation of both proteins should have led to an abnormal activation of *RUNX1/SIN3A* target genes, leading to myelodysplasia. Even if haploinsufficiency was never reported for *SIN3A*, its role as a TS has been described in other tumors [4]. Notably, the *SIN3A* corepressor was known to interact with *RUNX1* [5], leading to the transcriptional inactivation of their target genes [6].

In cases 2 and 3, FISH indicated that *RUNX1* was interrupted within intron 7. Additionally, in case 4, a 600-kb deletion removed the 5' portion of *RUNX1* starting from intron 6 (Fig. 2a and Additional file 1: Table S1). In

all cases, *RUNX1* was joined with an opposite transcriptional orientation to intron 3 of *TCF12* (NM_003205), a basic helix-loop-helix transcription factor (Fig. 2b) fused with *MLL* in MDS [7] and recurrently mutated in myeloproliferative disorders [8]. Notably, in case 2, RT-qPCR indicated the downregulation of both *RUNX1* and *TCF12* (Fig. 2c) and IPA analysis disclosed significant deregulation of the AML pathway. The number of altered pathways was slightly higher than in case 1 (146 vs. 136) and mostly overlapped the previously described categories. Particularly, *RUNX1* was shown to control many differentially expressed genes involved in cell cycle regulation, inflammatory response, and transcription regulation (Additional file 8: Figure S3 and Additional file 9: Table S6).

We thus suggest a TS role for *TCF12* in myeloid disorders, as already described in colon carcinoma [9]. The concurrent inactivation of *RUNX1* and *TCF12* should mimic the same leukemogenic effect of the t(8;21) *RUNX1/CBFA2T1* fusion protein. E proteins, like *TCF12*,

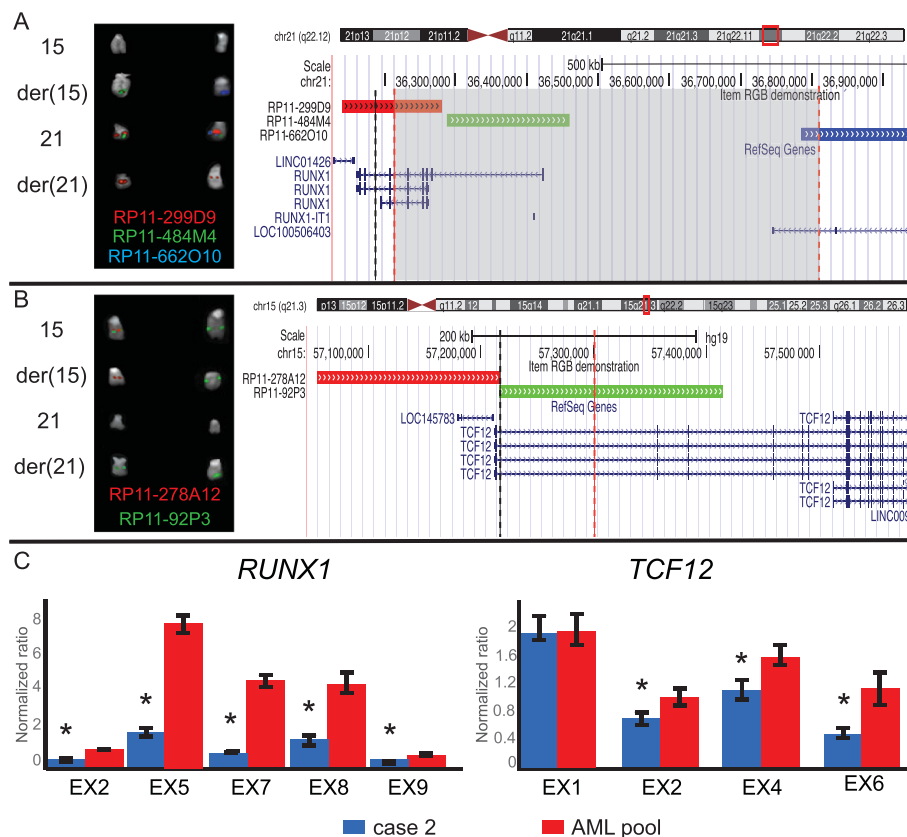


Fig. 2 t(15;21)(q21;q22) translocation in cases 2, 3, and 4. **a, b** Breakpoints on chromosomes 21 and 15: partial karyotypes showing fluorescence in situ hybridization (FISH) results that allowed the mapping of t(15;21) translocation breakpoints on der(21) (a) and der(15) (b), using the consistently colored probes listed for cases 2 (first column) and 4 (second column). RP11-662O10 was used only in case 4. Cases 2 and 3 shared the same breakpoints (data not shown). On the right, the map of the BAC probes used in the FISH experiments, according to GRCh37/hg19, and identifying both translocation and deletion breakpoints, is shown. The black and orange dashed lines indicate the breakpoints in cases 2 and 4, respectively. The grey rectangle encompasses the deleted region flanking the translocation breakpoint in case 4. **c** Evaluation of *RUNX1* and *TCF12* expression levels: exon-specific reverse transcription quantitative polymerase chain reaction results of runt-related transcription factor 1 (*RUNX1*; left) and transcription factor 12 (*TCF12*; right) in case 2. Asterisks indicate statistically significant results ($P < .05$)

are inactivated through their interaction with the domain TAFH of CBFA2T1, leading to the inhibition of the p300/CBP histone acetyltransferase recruitment at their target genes' promoters and consequently to the lack of activation of genes with E-box promoters [10].

To summarize, we here identified three novel *RUNX1* partner genes, including two transcription factors and a long noncoding RNA, in 2 t(15;21) translocations. Both of the t(15;21) translocations resulted in the concurrent inactivation of *RUNX1* and one related transcription factor (*SIN3A* or *TCF12*), leading to the potential haploinsufficiency of both involved genes. Moreover, the IPA analyses clearly indicated that the AML pathway was significantly deregulated in our samples, and showed that *RUNX1*, *SIN3A*, or *TCF12* have a crucial impact on differentially expressed genes. The analysis of additional cases harboring t(15;21) translocations will be helpful to better understand the pathogenetic impact of these alterations in myeloid neoplasms.

Ethics approval

This study was performed in agreement with the Declaration of Helsinki, and approved by the Ethical Committee at the "S. Martino" hospital, Belluno (Italy); Centre Hospitalier Universitaire Vaudois CHUV, Lausanne (Switzerland); University Hospital Leuven, (Belgium).

Consent for publication

Written informed consent was obtained from the patients for publication of this letter.

Additional files

Additional file 1: Table S1. Cytogenetic and clinical features of the patients included in the study. (DOCX 8 kb)

Additional file 2: Table S2. FISH results obtained with BAC and fosmid probes in all the cases included in the study. (DOCX 125 kb)

Additional file 3: Figure S1. FISH mapping of the t(15;21) translocation breakpoints in case 1. (A, B) Merged pseudocolored fluorescence in situ hybridization (FISH) results obtained with consistently colored BAC and fosmid probes spanning runt-related transcription factor 1. (C) Map of the probes used in the FISH experiments in panels A and B. The black dashed line indicates the breakpoint within the gene. (D, E) FISH results obtained with BAC and fosmid probes used to map the proximal (D) and distal breakpoints (E) on chromosome 15. (F) Map of the probes used in the FISH experiments, identifying both translocation and deletions breakpoints. Black dashed lines indicate the breakpoints; the grey rectangle encompasses the deleted region flanking the translocation breakpoint. (EPS 3237 kb)

Additional file 4: Table S3. SNP array results [EMBL: E-MTAB-3782] obtained in case 1. (DOCX 123 kb)

Additional file 5: Table S4. List of primers used for RT-PCR, RT-qPCR and Sanger sequencing. (DOC 91 kb)

Additional file 6: Table S5. Case 1 Chimerascan output: in bold the fusion genes validated by RT-PCR and Sanger sequencing. Case 2 Chimerascan output. (XLSX 309 kb)

Additional file 7: Figure S2. Expression pattern analysis of *UBL7-AS1* in case 1. Exon-specific reverse transcription quantitative polymerase chain reaction analysis of *UBL7-AS1* in case 1 vs a control pooled sample of

patients with acute myeloid leukemia. Asterisks indicate statistically significant results ($P < .05$). (EPS 246 kb)

Additional file 8: Figure S3. The IPA acute myeloid leukemia signaling pathway for cases 1 and 2. Orange and blue glyphs indicate genes with predicted enhanced or reduced activity, respectively. Green symbols represent downregulated genes. Equally, orange and blue toothed wheels stand for activated or inhibited biological processes. Case 1 differs from case 2 for its overall activation z-scores (3.5 vs 2.5). IPA, Ingenuity pathway analysis. (JPG 3319 kb)

Additional file 9: Table S6. IPA analysis results obtained in case 1. IPA analysis results obtained in case 2. (XLS 232 kb)

Abbreviations

AML: acute myeloid leukemia; FISH: fluorescence in situ hybridization; IPA: Ingenuity pathway analysis; MDS: myelodysplastic syndromes; PCR: polymerase chain reaction; RT-PCR: reverse transcription polymerase chain reaction; RT-qPCR: reverse transcription quantitative polymerase chain reaction.

Competing interests

The authors declare that they have no competing interests.

Authors' contributions

ALA performed bioinformatics analysis, analyzed all data, and wrote the paper; DT performed FISH analyses, molecular experiments and wrote the paper; FDA and AL performed FISH analyses; CLC, DM, JS, PV, and AVH prepared samples for FISH and molecular analyses, and provided clinical data of the patients; OP and MC performed SNP array CGH analysis; TM performed bioinformatics analysis; CTS reviewed all the data, and wrote the manuscript. All authors read and approved the final manuscript.

Funding

This work was supported by Associazione Italiana Ricerca sul Cancro (AIRC MFAG2011 No.11405 to CTS).

Author details

¹Department of Biology, University of Bari, Bari, Italy. ²UO Anatomia Patologica, Ospedale S. Martino, Belluno, Italy. ³Unité de génétique du cancer, Service de génétique médicale, Centre Hospitalier Universitaire Vaudois CHUV, Lausanne, Switzerland. ⁴Center for Human Genetics and Department of Hematology, University Hospital Leuven and KU Leuven, Leuven, Belgium. ⁵Department of Haematology, AZ Sint-Jan AV, Brugge, Belgium. ⁶Medical Genetics Unit, IRCCS Casa Sollievo della Sofferenza Hospital, San Giovanni Rotondo, Italy. ⁷IRCCS Casa Sollievo della Sofferenza, Mendel Institute, San Giovanni Rotondo, Italy.

Received: 16 October 2015 Accepted: 11 December 2015

Published online: 16 December 2015

References

- De Braekeleer E, Douet-Guilbert N, Morel F, Le Bris MJ, Ferec C, De Braekeleer M. *RUNX1* translocations and fusion genes in malignant hemopathies. *Future Oncol*. 2011;7:77–91.
- Giguere A, Hebert J. Identification of a novel fusion gene involving *RUNX1* and the antisense strand of *SV2B* in a BCR-ABL1-positive acute leukemia. *Genes Chromosomes Cancer*. 2013;52:1114–22.
- Ingenuity Pathway Analysis IPA® QRC. <http://www.qiagen.com/ingenuity>.
- Suzuki H, Ouchida M, Yamamoto H, Yano M, Toyooka S, Aoe M, et al. Decreased expression of the *SIN3A* gene, a candidate tumor suppressor located at the prevalent allelic loss region 15q23 in non-small cell lung cancer. *Lung Cancer*. 2008;59:24–31.
- Hu Z, Gu X, Baraoidan K, Ibanez V, Sharma A, Kadkol S, et al. *RUNX1* regulates corepressor interactions of PU.1. *Blood*. 2011;117:6498–508.
- Lutterbach B, Westendorf JJ, Linggi B, Isaac S, Seto E, Hiebert SW. A mechanism of repression by acute myeloid leukemia-1, the target of multiple chromosomal translocations in acute leukemia. *J Biol Chem*. 2000;275:651–6.
- Meyer C, Kowarz E, Yip SF, Wan TS, Chan TK, Dingermann T, et al. A complex MLL rearrangement identified five years after initial MDS diagnosis results in out-of-frame fusions without progression to acute leukemia. *Cancer Genet*. 2011;204:557–62.

8. Tenedini E, Bernardis I, Artusi V, Artuso L, Roncaglia E, Guglielmelli P, et al. Targeted cancer exome sequencing reveals recurrent mutations in myeloproliferative neoplasms. *Leukemia*. 2014;28:1052–9.
9. Starr TK, Allaei R, Silverstein KA, Staggs RA, Sarver AL, Bergemann TL, et al. A transposon-based genetic screen in mice identifies genes altered in colorectal cancer. *Science*. 2009;323:1747–50.
10. Park S, Chen W, Cierpicki T, Tonelli M, Cai X, Speck NA, et al. Structure of the AML1-ETO eTAFH domain-HEB peptide complex and its contribution to AML1-ETO activity. *Blood*. 2009;113:3558–67.

Submit your next manuscript to BioMed Central
and we will help you at every step:

- We accept pre-submission inquiries
- Our selector tool helps you to find the most relevant journal
- We provide round the clock customer support
- Convenient online submission
- Thorough peer review
- Inclusion in PubMed and all major indexing services
- Maximum visibility for your research

Submit your manuscript at
www.biomedcentral.com/submit

